THE 3-RPRR KINEMATICALLY REDUNDANT PLANAR PARALLEL MANIPULATOR

Iman Ebrahimi[1], Juan A. Carretero[2], Roger Boudreau[3]

[1] *Department of Mechanical Engineering, University of New Brunswick, Iman.Ebrahimi@unb.ca*

[2] *Department of Mechanical Engineering, University of New Brunswick, Juan.Carretero@unb.ca*

[3] *Département de génie mécanique, Université de Moncton, Roger.A.Boudreau@umoncton.ca*

Abstract

In this work, the 3-RPRR, a new kinematically redundant planar parallel manipulator with six degrees of freedom, is presented. First the manipulator is introduced and its inverse displacement problem discussed. Then, all types of the singularities of the 3-RPRR manipulator are analysed and demonstrated. Thereafter, the reachable and dexterous workspaces are obtained and compared with those of the non-redundant 3-PRR manipulator. Finally, based on a geometrical measure of proximity to singular configurations, actuation schemes for the manipulators are obtained. It is shown that the proposed manipulator is capable of following a path while avoiding the singularities.

Keywords: kinematic redundancy, planar parallel manipulators, inverse displacement, singularity analysis, workspace analysis, path planning

MANIPULATEUR PARALLÈLE PLAN REDONDANT DE TYPE 3-RPRR

Résumé

Cet article propose un nouveau manipulateur parallèle plan redondant ayant une architecture de type 3-RPRR qui comporte six degrés de liberté. L'architecture du manipulateur est présentée et le problème géométrique inverse est résolu. Tous les types de singularités du manipulateur 3-RPRR sont analysés et démontrés. Les espaces de travail atteignable et dextre sont ensuite obtenus pour le 3-RPRR et comparés avec ceux du manipulateur non redondant de type 3-PRR. Finalement, une stratégie d'actionnement est développée basée sur une mesure géométrique qui indique la proximité d'une configuration singulière. Il est démontré que le manipulateur proposé peut éviter les configurations singulières lorsqu'il suit une trajectoire.

Mots clés: redondance cinématique, manipulateur parallèle plan, analyse de singularités, problème géométrique inverse, espace de travail, planification de trajectoire

1 INTRODUCTION

Parallel manipulators have been broadly studied. Certain characteristics, when compared to serial manipulators, such as high payload-to-weight ratio, high rigidity, high accuracy and high-speed motion have made them useful mechanisms for certain applications. On the other hand, they suffer from relatively small workspaces, complex kinematics, low maneuverability and a high number of singular configurations. Many research have been conducted on improving the capabilities of parallel manipulators [1]. The majority of studies on parallel manipulators have concentrated on non-redundant manipulators. Redundancy in parallel manipulators, unlike serial manipulators [2; 3], has only been introduced in [4] and [5]. Redundancy can be divided into actuation redundancy and kinematic redundancy. *Actuation redundancy* can be explained as replacing existing passive joints of a manipulator by active ones. Consequently, actuation redundancy does not change the mobility or workspace of a manipulator but may cause singularity reduction [6]. *Kinematic redundancy*, on the other hand, adds to the mobility and degrees of freedom (DOF) of parallel manipulators. Kinematic redundancy occurs when extra active joints and links (if needed) are added to manipulators. As a result, kinematically redundant manipulators need more controlling variables than needed for a set of specified tasks [6].

In the present work, the 3-$\underline{\text{RP}}$RR[4], a new 6-DOF kinematically planar parallel manipulator is introduced first and its inverse displacement problem (IDP) is explained and illustrated. Then, Jacobian matrices of the manipulator are derived and all types of its kinematic singularities are obtained and their geometrical interpretations illustrated. Thereafter, the reachable and dexterous workspaces of the 3-$\underline{\text{RP}}$RR manipulator are compared to those of its original non-redundant 3-$\underline{\text{P}}$RR manipulator. Next, a geometrical method is proposed to measure the closeness of both the 3-$\underline{\text{RP}}$RR and the 3-$\underline{\text{P}}$RR manipulators to singular configurations. Using this measure as a cost function, a local optimisation method is used to illustrate how to determine the optimal actuation scheme.

2 PROPOSED ARCHITECTURES

The proposed kinematically redundant parallel manipulator originates from the non-redundant 3-$\underline{\text{P}}$RR planar parallel manipulators proposed in [7]. Considering Figure 1, if each limb of the illustrated manipulator has angles θ_i fixed, the resulting manipulator would be a 3-$\underline{\text{P}}$RR. That is, the 3-$\underline{\text{P}}$RR would have a prismatic actuator at point A_i, followed by two passive revolute joints at points D_i and B_i. The addition of the active revolute joint at A_i turns the manipulator into the depicted 3-$\underline{\text{RP}}$RR redundant planar manipulator. Note that throughout the present work, the solid circles in the figures represent active revolute joints whereas empty ones represent passive joints. Also note that throughout this work, $i = 1, 2, 3$. As for the 3-$\underline{\text{PR}}$RR manipulator studied in [9], adding one degree of kinematic redundancy (1-DOKR) to each limb not only reduces the singularities but also improves the workspace of the manipulator. Having the actuators at the base of the manipulator has the advantage of lessening the dynamic effects.

[4]The terminology used is the following. A 3-$\underline{\text{RP}}$RR mechanism indicates that the end-effector is connected to the base by three serial kinematic chains (limbs), each consisting of two active (and therefore underlined) joints, one revolute joint (R) and one prismatic joint (P), respectively, connected to the base, followed by two passive revolute joints, the second of which connects the limb to the end-effector.

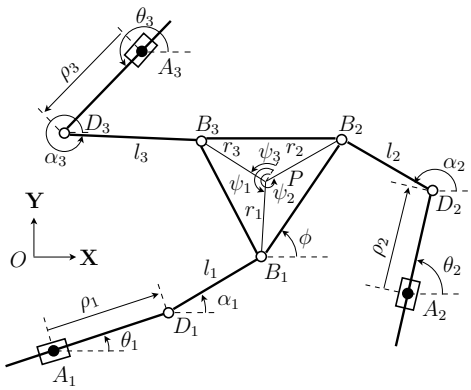

Figure 1: 3-RPRR planar 6-DOF kinematically redundant parallel manipulator (if θ_is were fixed, the manipulator would be 3-PRR).

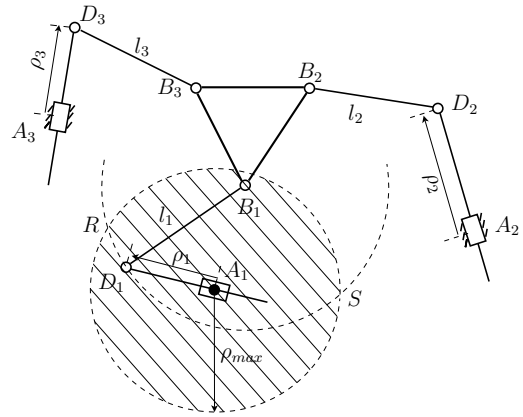

Figure 2: 4-DOF kinematically redundant planar parallel manipulator and its locus of solutions for the inverse displacement problem.

3 Inverse Displacement of Redundant Parallel Manipulators

Kinematic redundancy in parallel manipulators results in increasing the number of solutions for the IDP. More particularly, for a given pose of the end-effector inside the workspace, there are an infinite number of solutions. The IDP in kinematically redundant parallel manipulators results in a locus of solutions for each limb as opposed to a finite number of solutions in non-redundant parallel manipulators. Figure 2 shows a planar parallel manipulator which has 1-DOKR in its first limb. Considering limb A_iD_i, point D_1 can be anywhere on the hatched circle centred at point A_1. The radius of the circle is equal to the maximum displacement of the prismatic actuator. For a given position and orientation of the end-effector, link B_1D_1 can fully rotate around point B_1. Therefore, the locus of IDP solutions is the arc $\widehat{RD_1S}$.

Based on quantities shown in Figure 1, the inverse displacement solution of the 3-RPRR can be written as:

$$\overline{D_iB_i} = \overline{OP} + \overline{A_iO} + \overline{D_iA_i} + \overline{PB_i} \tag{1}$$

$$l_i^2 = (x_p - x_{A_i} - \rho_i c_{\theta_i} + r_i c_{(\phi+\psi_i)})^2 + (y_p - y_{A_i} - \rho_i s_{\theta_i} + r_i s_{(\phi+\psi_i)})^2 \tag{2}$$

$$l_i^2 = {x_{l_i}}^2 + {y_{l_i}}^2 = (l_i c_{\alpha_i})^2 + (l_i s_{\alpha_i})^2 \tag{3}$$

where $c_\measuredangle$ and $s_\measuredangle$ represent $\cos(\measuredangle)$ and $\sin(\measuredangle)$, respectively.

4 Singularity analysis

Jacobian matrices transform the velocity vector of the active joints in the velocity vector of the end-effector and vice-versa:

$$\mathbf{J_x}\dot{\mathbf{x}} = \mathbf{J_q}\dot{\mathbf{q}} \tag{4}$$

where $\dot{\mathbf{q}}$ is the velocity vector of the associated active joints and $\dot{\mathbf{x}}$ is the velocity vector of the end-effector. Considering equation (4), three types of singularities can be defined for parallel manipulators [8]:

1. Direct kinematic singularities when $\mathbf{J_x}$ is singular.

2. Inverse kinematic singularities when $\mathbf{J_q}$ is singular.

3. Combined (complex) singularities when $\mathbf{J_x}$ and $\mathbf{J_q}$ are singular.

Direct singularities take place when the determinant of $\mathbf{J_x}$ is zero ($|\mathbf{J_x}| = 0$), which means there are some nonzero velocities of the end-effector that cause zero velocities for the actuators. Conversely, inverse singularities ($|\mathbf{J_q}| = 0$) happen when there exist some nonzero actuator velocities that cause zero velocities for the end-effector.

4.1 Jacobian matrices of the 3-PRR and 3-RPRR manipulators

By selecting $\mathbf{x_r} = [x_p, y_p, \phi]^T$ and $\mathbf{q_r} = [\rho_1, \theta_1, \rho_2, \theta_2, \rho_3, \theta_3]^T$ as the displacement vectors for the end-effector and the actuators of the redundant manipulator, respectively, and differentiating equation (2) with respect to time, the Jacobian matrices in equation (4) become:

$$\mathbf{J_{x_r}} = \begin{bmatrix} a_{11} & a_{12} & a_{13} \\ a_{21} & a_{22} & a_{23} \\ a_{31} & a_{31} & a_{33} \end{bmatrix}_{3\times 3} \qquad \mathbf{J_{q_r}} = \begin{bmatrix} u_1 & v_1 & 0 & 0 & 0 & 0 \\ 0 & 0 & u_2 & v_2 & 0 & 0 \\ 0 & 0 & 0 & 0 & u_3 & v_3 \end{bmatrix}_{3\times 6} \tag{5}$$

where

$$\begin{aligned} a_{i1} &= x_p - x_{A_i} - \rho_i c_{\theta_1} + r_i c_{(\phi+\psi_i)} & u_i &= c_{\theta_i} a_{i1} + s_{\theta_i} a_{i2} \\ a_{i2} &= y_p - y_{A_i} - \rho_i s_{\theta_1} + r_i s_{(\phi+\psi_i)} & v_i &= -\rho_i s_{\theta_i} a_{i1} + \rho_i c_{\theta_i} a_{i2} \\ a_{i3} &= -r_i s_{(\phi+\psi_i)} a_{i1} + r_i c_{(\phi+\psi_i)} a_{i2} \end{aligned}$$

The displacement vectors of the end-effector and actuators of the 3-PRR are $\mathbf{x} = [x_p, y_p, \phi]^T$ and $\mathbf{q} = [\rho_1, \rho_2, \rho_3]^T$, respectively.

It should be noted that considering θ_i are fixed, $\mathbf{J_x}$ for the 3-PRR is the same as $\mathbf{J_{x_r}}$, but $\mathbf{J_q}$ is:

$$\mathbf{J_q} = \begin{bmatrix} u_1 & 0 & 0 \\ 0 & u_2 & 0 \\ 0 & 0 & u_3 \end{bmatrix}_{3\times 3} \tag{6}$$

4.2 Direct kinematic singularities of the 3-PRR and 3-RPRR manipulators

The direct kinematic singularities of planar parallel manipulators with architectures whose distal links have passive revolute joints at both ends such as the 3-PRR and 3-RPRR manipulators are the same. They all occur when the lines collinear with the distal links meet at a common point. The reason for this is that forces can only be transmitted in the distal link directions. Therefore, when all of them meet at a common point, while all the actuators are locked, the end-effector cannot sustain a moment applied to the end-effector.

The 3-PRR manipulator has only up to two solutions of the IDP for a given pose. On the other hand, as explained earlier for the 3-RPRR manipulator, it is possible to select any of the solutions for the inverse displacement of a kinematically redundant limb that are not in direct singularities

and avoid a considerable number of direct singularities. Therefore, adding 1-DOKR to the 3-PRR manipulator can reduce considerably the number of direct singularities of the 3-RPRR planar manipulator but not all of them [6]. By adding 2-DOKR it is possible to avoid all direct singularities for most manipulators [9]. Since there are two loci of solutions for two of the limbs it is possible to pick at least one that is not singular. Adding 1-DOKR to each limb of the 3-PRR not only makes the created kinematically redundant manipulator symmetrical but also improves its workspace and maneuverability. Therefore, the 3-RPRR manipulator has 6-DOF.

Based on equations (2) and (3), the direct Jacobian matrix of the 3-RPRR manipulator can be shown as:

$$\mathbf{J_{x_r}} = \begin{bmatrix} l_1 c_{\alpha_1} & l_1 s_{\alpha_1} & l_1 r_1 s_{(\alpha_1-\phi-\psi_1)} \\ l_2 c_{\alpha_2} & l_2 s_{\alpha_2} & l_2 r_2 s_{(\alpha_2-\phi-\psi_2)} \\ l_3 c_{\alpha_3} & l_3 s_{\alpha_3} & l_3 r_3 s_{(\alpha_3-\phi-\psi_3)} \end{bmatrix}_{3\times 3} \tag{7}$$

The determinant of $\mathbf{J_{x_r}}$ is zero when there are linear dependencies between any two or more rows or columns. That is,

$$\lambda_1 \mathbf{\Gamma}_1 + \lambda_2 \mathbf{\Gamma}_2 + \lambda_3 \mathbf{\Gamma}_3 = 0 \tag{8}$$

where λ_i are the coefficients of linear dependency which more than two λ_is cannot be zero simultaneously. Vector $\mathbf{\Gamma_i}$ represents the ith row or column of $\mathbf{J_{x_r}}$. Having only one λ_i nonzero, associates with cases that one row or column is zero. Considering equation (7), the elements of the first or second columns are zeros, when $c_{\alpha_i} = 0$ or $s_{\alpha_i} = 0$, respectively. These two conditions happen when all the distal links of the 3-RPRR manipulator become parallel and are also parallel to the *Y* or *X* axes, respectively. In both cases, the distal links are said to meet at a common point at infinity. Note that singularities do not depend on the chosen coordinate system. Thus, the singularity conditions described above can be expanded to the distal links being parallel regardless of their alignment with any of the axes. For the 3-RPRR manipulator, singular configurations only depend on relative positions and orientations of the distal links.

The third column becomes zero when all three distal links meet at point P. Again, since singularities are not frame dependent,the direct singularities can take place when all the distal links meet at a common point, shown in Figure 3a.

Linear dependency between the rows have the same meaning as between the columns. Linear dependency between any two rows happens when two distal links are aligned with the side of the end-effector that is between them. Figure 3b illustrates such a configuration for the first and second limb. Since for this configuration $\alpha_1 = \alpha_2 - \pi = \phi$ the direct Jacobian $\mathbf{J_{x_r}}$ in equation (7) can be written as:

$$\mathbf{J_{x_r}} = \begin{bmatrix} l_1 c_{\alpha_1} & l_1 s_{\alpha_1} & -l_1 r_1 s_{\psi_1} \\ -l_2 c_{\alpha_1} & -l_2 s_{\alpha_1} & l_2 r_2 s_{\psi_2} \\ l_3 c_{\alpha_3} & l_3 s_{\alpha_3} & l_3 r_3 s_{(\alpha_3-\phi-\psi_3)} \end{bmatrix}_{3\times 3} \tag{9}$$

Considering Figure 3b, it is evident that $r_1 s_{\psi_1} = r_2 s_{\psi_2}$, therefore, the first and second rows are linearly dependent. The same can be shown for any other two limbs of the 3-RPRR. This linear dependency like the one for the columns is independent from the fixed and moving coordinate systems. The same discussion can be given for the 3-PRR non-redundant manipulator.

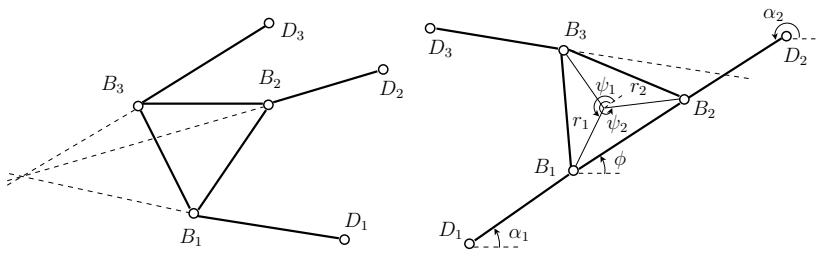

a) columns linear dependency b) rows linear dependency

Figure 3: Examples of direct singularities for the 3-RPRR manipulator with linear dependency between columns/rows.

4.3 Inverse kinematic singularities of the 3-PRR and 3-RPRR manipulators

For redundant parallel manipulators, inverse singularities occur when the determinant of $\mathbf{J_{q_r}}\mathbf{J_{q_r}}^T$ is zero [1]. It implies that inverse singularities take place when all the non-redundant manipulators, extracted by freezing three of the active joints from the 3-RPRR are in singularity.

$$\mathbf{J_{q_r}}\mathbf{J_{q_r}}^T = \begin{bmatrix} u_1^2+v_1^2 & 0 & 0 \\ 0 & u_2^2+v_2^2 & 0 \\ 0 & 0 & u_3^2+v_3^2 \end{bmatrix}_{3\times 3} \qquad u_i = l_i c_{(\alpha_i-\theta_i)} \quad v_i = l_i \rho_i s_{(\alpha_i-\theta_i)} \tag{10}$$

$|\mathbf{J_q}\mathbf{J_q}^T|$ is zero when any diagonal elements or all of them are zeros. For each limb to be in inverse singularities, both of the following conditions must be satisfied:

$$\rho_i = 0 \quad AND \quad \alpha_i = (\tfrac{2n+1}{2})\pi + \theta_i \quad n = 0, 1, 2, ...$$

These conditions mean that inverse singularities take place when length A_iD_i is zero (*i.e.*, $\rho_i = 0$) and D_iB_i is perpendicular to the direction of the prismatic actuator. Therefore, by avoiding the ρ_is to approach zero values while α_i relative to θ_i approaches a right angle, it is possible to avoid inverse singularities for the redundant 3-RPRR manipulator. Figure 4a illustrates a configuration when the third limb of the 3-RPRR manipulator is in an inverse kinematic singularity.

According to Equation (6), inverse singularities take place for the non-redundant 3-PRR manipulator, when any or all of the terms u_i are zeros. Hence, the 3-PRR is in inverse singularities when D_iB_i is perpendicular to A_iD_i. Figure 4b illustrates a configuration when the first limb is in an inverse singularity.

4.4 Combined (complex) singularities of the 3-PRR and 3-RPRR manipulators

The combined singularities occur when both direct and inverse kinematic singularities take place. In other words, when both $\mathbf{J_{x_r}}$ and $\mathbf{J_{q_r}}\mathbf{J_{q_r}}^T$ (for the non-redundant manipulator $\mathbf{J_x}$ and $\mathbf{J_q}$) are singular. Figures 4c and 4d show configurations in which both direct and inverse singularities occur at the same time for both manipulators. For the 3-RPRR manipulator this means the lines passing through all three D_iB_i links meet at a common point and one or more branches (branch three in Figure 4c) satisfy the condition described above where D_iB_i is perpendicular to A_iD_i while $\rho_i = 0$. The same conditions are necessary for the 3-PRR manipulator to be at a combined singularity except for the fact that ρ_i does not need to be zero (see Figure 4d).

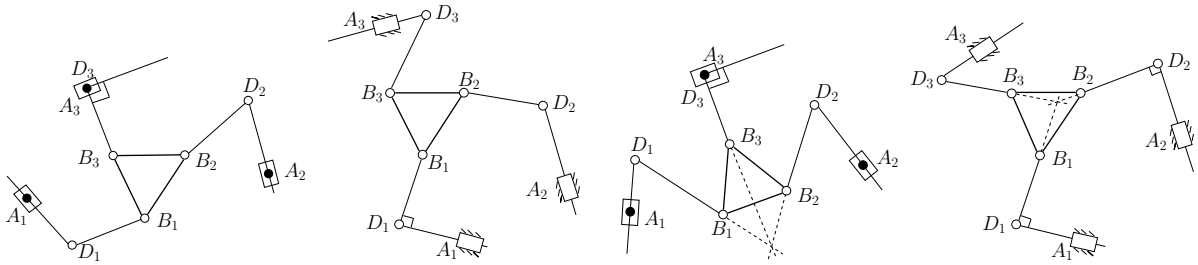

a) 3-RPRR b) 3-PRR c) 3-RPRR d) 3-PRR

Figure 4: Example of geometrical interpretation of singularities: a,b) inverse kinematic singularities, c,d) combined kinematic singularities.

Table 1: Workspace comparison for the 3-PRR and 3-RPRR. All absolute quantities are in m^2.

	Reachable		Dexterous		Ratio
	Abs.	Rel.	Abs.	Rel.	$\frac{Dexterous}{Reachable}$
3-PRR	0.381	1	0.199	1	0.522
3-RPRR	1.555	4.080	1.078	5.417	0.693

5 WORKSPACE ANALYSIS

Workspace analysis in the present work is based upon two types of workspaces: reachable and dexterous. The reachable workspace is defined as the region that the end-effector can reach with at least one orientation of the end-effector. Therefore, when a solution for the inverse displacement problem for a given point exists, that point is said to be in the reachable workspace. The dexterous workspace on the other hand, is defined as a region of the reachable workspace that the end-effector can reach with all possible orientations [1]. Here, the workspace of the manipulators are obtained by discretizing the area and finding whether the inverse displacement solution exists or not for each point in the discretized region.

The geometric parameters of the 3-PRR and the 3-RPRR manipulators based on Figure 1 are: $A_1A_2 = A_2A_3 = A_3A_1 = 1.0$ m, $B_1B_2 = B_2B_3 = B_3B_1 = 0.10$ m, $r_i = 0.0577$ m, $l_i = 0.30$ m, $\psi_1 = \frac{7\pi}{6}$, $\psi_2 = \frac{11\pi}{6}$, $\psi_3 = \frac{\pi}{2}$, $\rho_i^{max} = 0.866$ m and $\rho_i^{min} = 0$ m. Table 1 lists the absolute and relative areas (written as Abs. and Rel., respectively) of the reachable and dexterous workspaces of the 3-RPRR relative to that of the 3-PRR. Both reachable and dexterous workspaces of the redundant 3-RPRR manipulator are considerably larger than for the non-redundant 3-PRR manipulator. Also, the ratio of the dexterous workspace relative to the reachable workspace has improved considerably in the redundant manipulator.

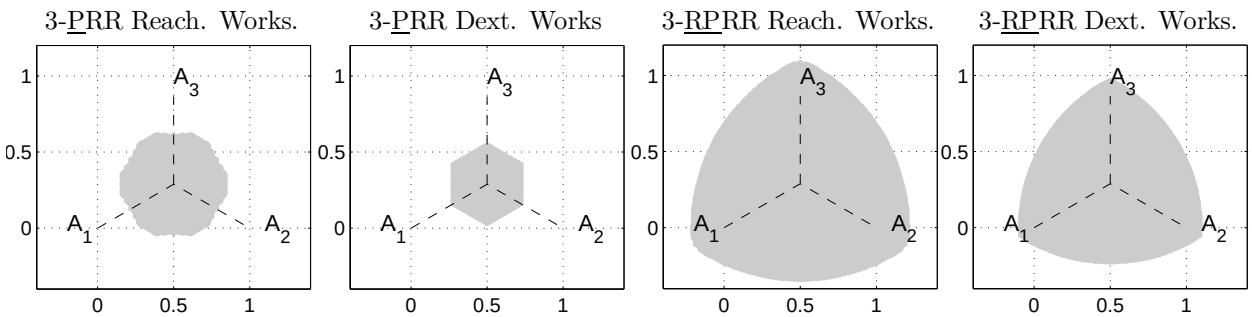

Figure 5: Workspace comparison between the 3-PRR (non-redundant) and the 3-RPRR (redundant) planar parallel manipulators.

6 Actuation Scheme for the 3-PRR and 3-RPRR manipulators

One of the reasons of the analysis of a mechanism from the point of the IDP, singularities and workspace is path planning and eventually determining an actuation scheme for it. Adding kinematic redundancy to a mechanism makes the planning and controlling tasks more challenging. The reason is that there are more independent variables for a kinematically redundant manipulator than for a non-redundant one. On the other hand, using kinematic redundancy can help avoid some or all of singularities and also enlarge the workspace [6; 9].

Here, the 3-RPRR and the 3-PRR manipulators are compared in terms of their performance while following an arbitrary path. As aforesaid, kinematic redundancy increases the number of inverse displacement solutions for each limb from a limited number of solutions (here up to two solutions for the 3-PRR) to a locus of solutions. Therefore, it is necessary to apply a method to choose a solution from all possible solutions. Here a method is proposed based on a geometrical measurement.

6.1 Normalised scaled incircle radius (NSIR)

As shown in the direct singularity analysis of the 3-RPRR manipulator, these configurations occur when the lines collinear to distal links meet at a common point. Since direct singularities only depend on the distal links, inverse singularities for the 3-PRR are the same as for the 3-RPRR. One way to measure the closeness of the manipulator to direct singularities is to measure the radius of the incircle[5] associated with the triangle created by the three lines passing through the distal links, as shown in Figure 6.

Assuming there are three points and that there are three lines constrained to pass through them. It can be shown that the largest incircle radius of any triangle created by those three lines cannot be larger than the circle that passes through those three fixed points. This makes the largest radius of the incircle a finite and known value. As a result, it is possible to normalise the incircle radius for any manipulator configuration by dividing the current radius by the maximum incircle radius. Measuring incircle radius for measuring singularity closeness, originally was introduced in [10].

[5]In geometry, the incircle (or inscribed circle) of a triangle is the largest circle contained inside it and is tangent to the three sides of the triangle.

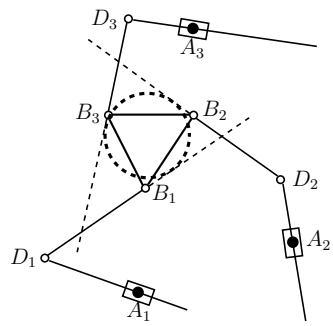

Figure 6: Incircle of the triangle created by the collinear lines passing through the distal links of the 3-RPRR manipulator.

Besides direct singularities, inverse singularities should be taken into account. Inverse singularities occur when $|\mathbf{J_q}| = 0$ for the 3-PRR manipulator and $|\mathbf{J_{q_r}}\mathbf{J_{q_r}}^T| = 0$ for the 3-RPRR manipulator. Since both $\mathbf{J_q}$ and $\mathbf{J_{q_r}}\mathbf{J_{q_r}}^T$ are diagonal, this condition can be written as:

$$\begin{aligned} |\mathbf{J_q}| &= \prod_{i=1}^{3} l_i c_{(\alpha_i - \theta_i)} \\ \sqrt{|(\mathbf{J_{q_r}})(\mathbf{J_{q_r}})^T|} &= \prod_{i=1}^{3} l_i \sqrt{(c_{(\alpha_i-\theta_i)})^2 + (\rho_i s_{(\alpha_i-\theta_i)})^2} \end{aligned}$$

The maximum value of $|\mathbf{J_q}|$ and $\sqrt{|(\mathbf{J_{q_r}})(\mathbf{J_{q_r}})^T|}$ are:

$$|\mathbf{J_q}|_{max} = \prod_{i=1}^{3} l_i \tag{11}$$

$$\sqrt{|(\mathbf{J_{q_r}})(\mathbf{J_{q_r}})^T|_{max}} = \begin{cases} \prod_{i=1}^{3} l_i & \rho_{max} \leq 1 \\ \prod_{i=1}^{3} l_i \rho_i & \rho_{max} > 1 \end{cases} \tag{12}$$

The maximum of $|\mathbf{J_q}|$ and $\sqrt{|(\mathbf{J_{q_r}})(\mathbf{J_{q_r}})^T|}$ help to define a coefficient for including the effects of the inverse Jacobian matrices.

Assume the lines collinear with the distal links intersect each other at three points called T_1, T_2 and T_3, and the sides of the triangle created are t_1, t_2 and t_3. Then, the incircle radius of the triangle created by the distal links can be obtained as:

$$A = \begin{vmatrix} x_{T_1} & y_{T_1} & 1 \\ x_{T_2} & y_{T_2} & 1 \\ x_{T_3} & y_{T_3} & 1 \end{vmatrix} \qquad r = \frac{A}{t_1+t_2+t_3} \tag{13}$$

If all three lines collinear with the distal links are parallel, the manipulator is in a singularity as mentioned before in the direct singularity analysis. When two out of three of these lines are parallel, the radius is half the distance of the two parallel lines. To take into consideration the

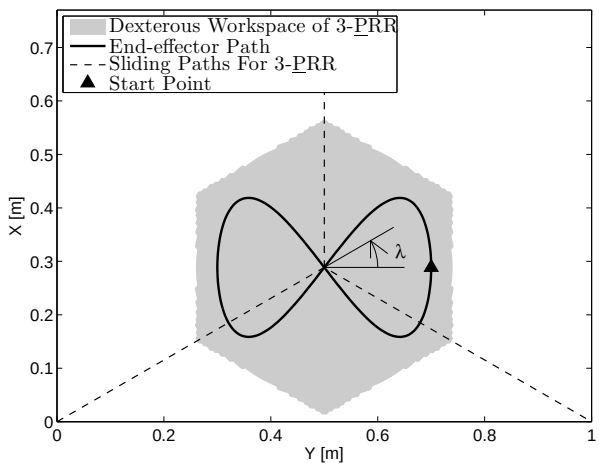

Figure 7: Specified path for the end-effector.

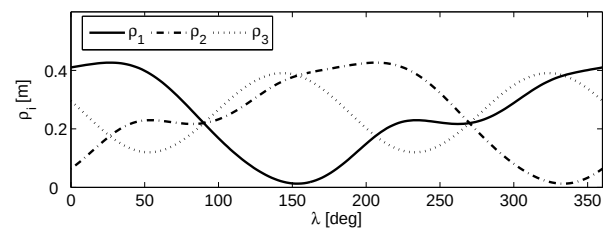

Figure 8: Prismatic actuation path ρ_i while tracking the path for the non-redundant 3-PRR.

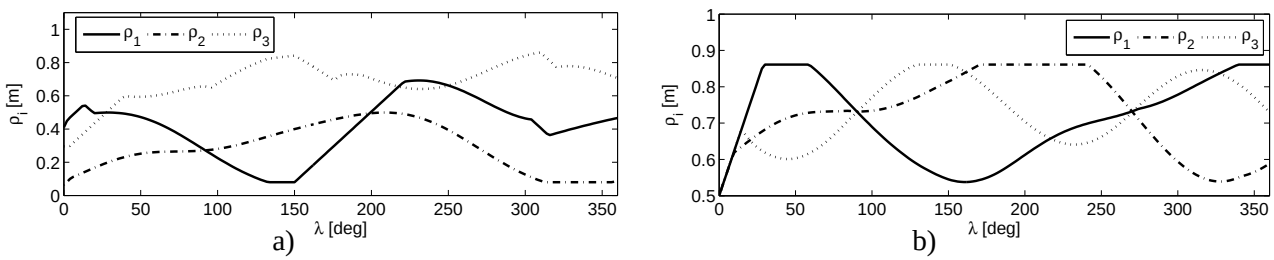

Figure 9: Prismatic actuation path ρ_i for the 3-RPRR with NSIR the method a) When the manipulator starts from the same configuration as the 3-PRR and b) When the manipulator starts from a different configuration than the 3-PRR.

closeness of the third line to be parallel to the first two, the radius is then multiplied by a coefficient defined as the distance of the two parallel lines over the length of the segment created by the intersection of two parallel lines with the non-parallel third line. Therefore, if the third line is perpendicular to the other two parallel lines, the coefficient is one. Conversely, when the three lines are close to being parallel, the coefficient would approach zero.

The coefficient of the ratio of the determinants of the inverse Jacobian can be defined as:

$$\begin{aligned} \xi &= \frac{|\mathbf{J_q}|}{|\mathbf{J_q}|_{\max}} \\ r_{scaled} &= \xi r \\ \mathcal{N}_r &= \frac{r_{scaled}}{r_{max}}\xi \qquad\qquad 0 \leq \mathcal{N}_r \leq 1 \end{aligned} \tag{14}$$

Similar equations can be written for the 3-RPRR manipulator.

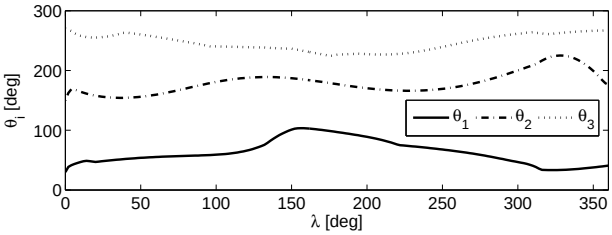

Figure 10: Actuation scheme of the revolute joints θ_i for the 3-RPRR manipulator tracking the path, when the manipulator starts from the same configuration as the 3-PRR.

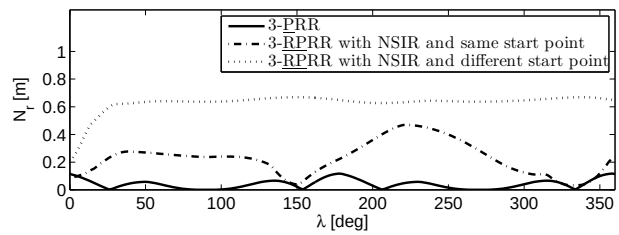

Figure 11: Normalised scaled incircle radius (NSIR) of the manipulators while tracking the path in Figure 7.

6.2 Results and Comparison

For any given pose for the end-effector, kinematic redundancy results in having loci of solutions for each limb of the 3-RPRR manipulator. Therefore, one set of solutions should be selected. Here for the 3-RPRR manipulator, the actuation scheme is based on maximising the NSIR as the cost function for each point along the path.

Figure 7 illustrates the path considered for both manipulators to follow. Figure 7 also shows that the chosen path is inside of the dexterous workspace of the non-redundant manipulator. Two scenario are considered, the first one is when the 3-RPRR manipulator starts at the same configuration as the 3-PRR. The second scenario is when the redundant manipulator starts at another configuration.

Figures 8, 9a and 9b show the prismatic actuations schemes for both manipulators as a function of angle λ used to define the cyclic path. Figure 10 illustrates the redundant revolute actuators' schemes for the 3-RPRR manipulator for the first scenario. Figure 11 illustrates the history of the NSIR ($\mathcal{N}_r$) of both manipulators while tracking the given path.

Based on Figure 11, for the redundant 3-RPRR manipulator for both scenario, $\mathcal{N}_r$ maintains a better value than the non-redundant manipulator. Also, if the 3-RPRR manipulator would not be forced to start from the same configuration as the non-redundant manipulator, the $\mathcal{N}_r$ value would improve even more. On the other hand, $\mathcal{N}_r$ for the non-redundant 3-PRR manipulator is close to zero throughout the entire path.

7 Conclusions

A new kinematically redundant planar parallel manipulator was proposed and its IDP was explained and illustrated. All types of singularities of the manipulator were analysed, illustrated and compared to those of the 3-PRR. It was shown that the proposed manipulator can avoid direct singularities by choosing different solutions for the IDP from the loci of solutions. Also, as long as none of the prismatic actuators are approaching a length of zero, it is possible to avoid the inverse singularities. It was also shown that both reachable and dexterous workspaces of the 3-RPRR manipulator are substantially larger than those of the non-redundant manipulator. Moreover, the ratio of the dexterous workspace over the reachable workspace is increased in the redundant ma-

nipulator. Finally, the actuation schemes of the two manipulators were studied for a given path. The results show that using kinematic redundancy considerably improves the characteristics of the manipulator by avoiding singularities. A geometrical measurement (NSIR) was proposed as a cost function to use in maximisation of the distance to singularities while generating the path. It was shown that even by using a local optimisation and using the NSIR as the cost function, it is possible to actuate the redundant manipulator in a way to avoid singularities.

REFERENCES

[1] J.-P. Merlet, Parallel robots, Springer, 2nd Edition, 2006.

[2] A. Maciejewski, C. Klein, Obstacle avoidance for kinematically redundant manipulators in dynamically varying environments, International Journal of Robotics Research 4 (3) (Fall 1985) 109–17.

[3] Y. Nakamura, H. Hanafusa, T. Yoshikawa, Task-priority based redundancy control of robot manipulators, International Journal of Robotics Research 6 (2) (Summer 1987) 3–15.

[4] S. Lee, S. Kim, Kinematic analysis of generalized parallel manipulator systems, Proceedings of the IEEE Conference on Decision and Control 2 (1993) 1097–1102.

[5] J.-P. Merlet, Redundant parallel manipulators, Laboratory Robotics and Automation 8 (1) (1996) 17–24.

[6] J. Wang, C. M. Gosselin, Kinematic analysis and design of kinematically redundant parallel mechanisms, Journal of Mechanical Design 126 (1) (2004) 109–118.

[7] C. Gosselin, S. Lemieux, J.-P. Merlet, A new architecture of planar three-degree-of-freedom parallel manipulator, Proceedings. 1996 IEEE International Conference on Robotics and Automation (Cat. No.96CH35857) vol.4 (1996) 3738–3743.

[8] C. M. Gosselin, J. Angeles, Singularity analysis of closed-loop kinematic chains, IEEE Transactions on Robotics and Automation 6 (3) (1990) 281–290.

[9] I. Ebrahimi, and J. A. Carretero and R. Boudreau. 3-PRRR redundant planar parallel manipulator: inverse displacement, workspace and singularity analyses. *Mechanism and Machine Theory*, doi:10.1016/j.mechmachtheory.2006.07.006., available online.

[10] I. Ebrahimi, J. A. Carretero, R. Boudreau, Path planning for the 3-PRRR redundant planar parallel manipulator, Accepted for publication in Proceedings of the 2007 IFToMM World Congress, IFToMM, Besançon, France, 2007.

[11] T. Yoshikawa, Foundations of Robotics: Analysis and Control, MIT, London, England, 1990.